Nonequilibrium Modeling of Condensed Mode Cooling of Polyethylene Reactors

Yan Jiang, Kim B. McAuley, and James C. C. Hsu
Dept. of Chemical Engineering, Queen's University, Kingston, Ontario, Canada K7L 3N6

In most industrial gas-phase polyethylene reactors, heat is removed by cooling the recycle gas stream in an external heat exchanger, where a portion of the vapor is condensed. The condensate evaporates in the reactor to absorb heat released by polymerization reactions, thereby increasing the production capacity of the unit. Nonequilibrium methods of multicomponent condensation are applied to develop a 1-D model to simulate the cooling unit of an industrial polyethylene reactor system operated in partial condensing mode. Finite difference approximations are used to convert the resulting set of differential equations to algebraic equations. A practical method of solving the equations is to combine the rapid local convergence of Newton's method with a globally convergent strategy. Correlation methods for estimating local heat-transfer coefficients in the liquid film layer are discussed. Butterworth's method for shear-stress-controlled condensate flow gives reasonable agreement between simulation results and industrial data, while Chen et al.'s method can better describe the transition process of condensate flow from laminar to turbulent flow.

Introduction

A large portion of polyethylene is produced in gas-phase fluidized-bed reactors. Since the polymerization reaction is highly exothermic, the primary limitation on reaction rate is the rate at which heat can be removed from the reaction zone (Jenkins et al., 1986). According to Choi and Ray (1985), the conversion per pass through the reactor is low (2–5%); hence, the recycle gas stream is much larger than the fresh feed. Therefore, the heat removal rate mainly depends on cooling of the recycle gas mixture in a heat-exchanger external to the reactor. In polyethylene reaction systems it is possible to operate in two different modes: noncondensing operation and condensing operation. One of the advantages of condensing mode operation is that it is possible to increase the heat removal capacity by use of latent heat of condensation and a greater temperature difference between the inlet gas temperature and reactor temperature, thereby increasing the production capacity of the unit of given size (Burdett, 1988). Today, condensing mode operation is a common practice in polyethylene industry. The typical recycle gas mixtures contain seven to eight gases including H_2 and N_2 (Jenkins et al., 1986), which are noncondensable under the operating conditions in polyethylene reactor systems. Hydrogen is a chain transfer agent used in polymerization. Nitrogen is used to carry the catalyst into the bed. The problem is that very little is known about the effects of operating conditions in the heat exchanger and reactor system on the heat removal rate. The objectives of this article are to apply nonequilibrium methods based on film theory to develop a model to describe multicomponent condensation processes in a vertical single pass shell-and-tube heat exchanger in a polyethylene reactor system in order to present effective numerical methods for solving the highly nonlinear model equations, to investigate the effects of heat-transfer resistance in the condensate liquid film at highly turbulent flow conditions, and to compare simulation results with industrial data.

Multicomponent condensation is a process of simultaneous heat and mass transfer. Since mass-transfer processes are much more complicated than heat transfer, they constitute the center of the matter. According to different approaches to describe mass transfer, existing methods for the analysis of the condensation of multicomponent mixtures are of two basic kinds: equilibrium methods and nonequilibrium methods. Nonequilibrium methods are classified into film methods and boundary layer methods.

In equilibrium methods, the condensation process is assumed to pass through a series of equilibrium states. In this class of methods (Kern, 1950; Silver, 1947; Bell and Ghaly, 1973), mass-transfer resistances in both the vapor and liquid

phases are ignored. Since equilibrium methods are simple and rapid in computation, they are favored methods for industrial design of multicomponent vapor condensers, and are best suited to describe totally condensable mixtures. In partial condensers where noncondensable species are present, the vapor composition leaving a partial condenser may differ substantially from that estimated assuming equilibrium between liquid and vapor phases.

More soundly based nonequilibrium methods using a film model (Colburn and Drew, 1937) have existed for binary mixtures for many years. Generalization of this film model to multicomponent mixtures is not straightforward, because diffusional interactions in the multicomponent systems may give rise to such phenomena as reverse diffusion, osmotic diffusion, and diffusion barriers. Due to wide application of multicomponent condensation in industrial practice, great interest has arisen for the development of generalized multicomponent mass-transfer methods in the past two decades (Schrodt, 1973; Krishna et al., 1976; Krishna and Panchal, 1977; Krishna, 1979; Krishna and Standart, 1979; Bandrowski and Kubaczka, 1981; Webb and Sardesai, 1981; Taylor and Noah, 1982). In film theory methods, primary consideration is given to heat and mass transfer in the vapor phase. Concentration and temperature differences between the bulk vapor and vapor-liquid interface are assumed to occur across a thin laminar film adjacent to the interface. The situation is idealized by assuming that the movement of the thin film layer is wholly laminar, and outside this film, there is a highly turbulent region in which the concentration and temperature gradients are negligible. Consequently, 1-D differential material and energy balance equations can be used to describe multicomponent condensation processes. There are a large number of methods that could be used to calculate the local mass-transfer rates in the vapor phase. The methods to calculate mass-transfer rates fall into three categories: (1) effective diffusivity methods (which neglect diffusion interaction effects); (2) methods that take interaction effects into account and which are implicit in calculating the molar fluxes N_i^V ($\text{kmol}\cdot\text{m}^{-2}\,\text{s}^{-1}$) such as the methods based on an exact solution of the Maxwell-Stefan equations (Krishna and Standart, 1976), and the solution of the linearized equations due to Toor (1964) and to Stewart and Prober (1964); and (3) simplified methods, such as those of Krishna (1979) and Taylor and Smith (1982), that take interaction into account, but are explicit in computing the molar fluxes. Many efforts have been made to investigate and compare these three kinds of methods. Experiments were carried out by Sardesai (1979), who investigated condensation of two vapor mixtures in the presence of a noncondensable gas. Numerical simulations of the experiments were discussed by Webb and Sardesai (1981) and McNaught (1983). Comparison of available experimental data and many design simulations has shown definite evidence for the significance of interactive effects in multicomponent condensation. In general, the various film models (including explicit methods) that take interaction effects into account give very similar results when used to predict the performance of a condenser. The effective diffusivity methods yield reasonably good predictions of the total condensation rates. However, these methods may result in a significantly over- or underdesigned condenser, and a quite poor estimation of compositions of each component in both liquid and vapor phases. There is no computational advantage for using effective diffusivity methods, and they are not recommended (Taylor and Krishna, 1993, p. 476). More detailed reviews are given by Taylor et al. (1986) and Taylor and Krishna (1993).

Boundary layer methods are more sophisticated nonequilibrium methods based on boundary layer theory. The analysis is based on a rigorous solution of mass, energy and momentum balance equations describing the vapor boundary layer and the condensate film. Extensive work has been done in condensation of binary mixtures to investigate effects of energy convective terms, interfacial shear stress, the presence of noncondensable gases and the turbulent flow of the vapor. Currently, boundary layer methods are still in the process of theoretical development. Applications are limited primarily to modeling the condensation of binary mixtures with simplified boundary conditions. Extensions to multicomponent systems are few in number (Taitel and Tamir, 1974; Tamir and Merchuk, 1979; Kholpanov and Kenig, 1993) and cannot be used for practical condensation calculations, because of the enormity of the computational procedure required.

Application to condensing mode operation

From the above analysis, the nonequilibrium methods based on film models are currently the most appropriate approach to describe multicomponent condensation processes. In polyethylene reactor systems, the recycle gas mixture enters either a vertical or a horizontal heat exchanger at a very high flow rate (Jenkins et al., 1986). In this article, we only focus on studying a vertical heat-exchanger arrangement in the reactor system. For partial condensation of a multicomponent mixture in such highly turbulent flow, there is little resistance to mass transfer in the bulk vapor phase of the fluid. Therefore, the assumptions of the film theory are quite reasonable. As a result, film theory methods are applied here to develop model equations. Although film theory methods are well developed for describing multicomponent mass-transfer processes, there is a great shortage of experimental data for heat and mass transfer in multicomponent vapor-liquid systems. Industrial data are sometimes excellent alternative sources that can be used to test a new theory or methods. Despite a number of existing design methods for multicomponent condensers, data regarding the application of nonequilibrium methods in industry are not available in the open literature. Since industrial situations are usually more complicated than simple design simulations, the amount of computation involved is expected to be significantly greater. In addition, many more model parameters must be specified. In their literature review, Kim and Corradini (1990) indicated that the presence of noncondensable gases and turbulent flow are the two most important factors affecting condensation heat transfer. One goal of the current investigation is to obtain better understanding of these issues.

Process description

Figure 1 shows a vertical shell-and-tube heat exchanger used in an industrial polyethylene reactor system. The recycle gas mixture flows downward on the tube side, and cooling water passes in countercurrent flow through the shell side. At

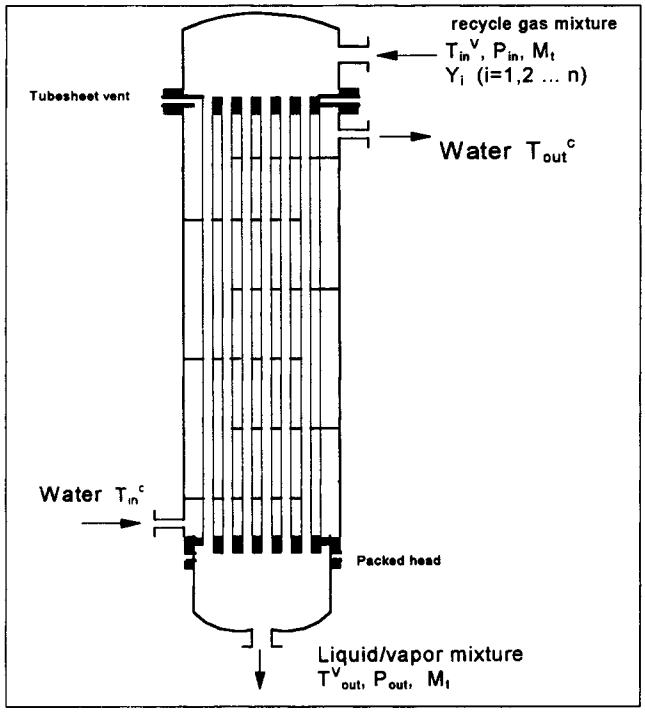

Figure 1. Vertical shell-and-tube heat exchanger.

the top of the exchanger, available measurements include inlet vapor temperature T_{in}^{V} (K), inlet pressure P_{in} (kPa), the mass-flow rate of the vapor mixture, the mole fraction of each component Y_i^V, and the outlet cooling water temperature T_{out}^{c}. At the bottom of the exchanger, the temperature of the vapor phase T_{out}^{V}, the outlet pressure P_{out}, and the inlet cooling water temperature T_{in}^{c} are also known. Condensation begins part of the way along the length of the heat exchanger. At the bottom of the exchanger, the amount of condensed liquid is around 20 wt. %. The exchanger can be operated at pressures ranging from 250–500 psig (1.7–3.4 MPa) (Jenkins et al., 1986).

Model Equations

Assuming constant pressure throughout the heat exchanger, 1-D material and energy balance equations combining the local heat- and mass-transfer rate equations constitute the mathematical model describing multicomponent condensation process. The local heat- and mass-transfer rate equations are obtained by applying film models. Given the conditions of the entering streams at position $j-1$ (the bulk vapor phase temperature T_{j-1}^{V}, molar flow rate of each component $V_{i,j-1}$, and the total molar flow rate of the vapor phase $m_{V,j-1}$; if the liquid phase exists, $L_{i,j-1}$ and $m_{L,j-1}$ must also be specified), and the conditions of the coolant side (temperature T_{j-1}^{c} and the flow rate), by solving the model equations for an increment of heat-exchanger length, one can determine the conditions of the vapor and liquid streams as well as the coolant at the next position j (T_j^V, T_j^I, T_j^W, T_j^c, $V_{1,j}$, ..., $V_{n,j}$, $N_{1,j}$, ..., $N_{n,j}$, L_{1j}, ..., L_{nj}, y_{1j}^I, ..., $y_{n-1,j}^I$). Continually solving the model equations in this way, the temperature and composition distributions of vapor and liquid streams along the length of the heat exchanger can be obtained. In the preceding list of $4n+3$ unknowns, T_j^I and T_j^W are vapor/liquid interface temperature and tube wall temperature respectively, N_{ij} is molar flux of species i, and y_{ij}^I is vapor mole fraction of species i at the vapor/liquid interface. The detailed method for determining the solutions is given below.

Conservation equations

We consider a 1-D gas-liquid cocurrent downward flow in a vertical tube as shown in Figure 2. The conservation of mass for the vapor and liquid phases within a short section of a tube can be expressed as

$$dm_V = -dm_L \tag{1}$$

where m_V and m_L are molar flow rates of the vapor and liquid (kmol·s^{-1}), respectively. The material balance for individual components in both liquid and vapor phases can be written as

$$\frac{dV_i}{dA} = -N_i^V \qquad i=1,2,\ldots n \tag{2}$$

$$\frac{dL_i}{dA} = N_i^L \qquad i=1,2,\ldots n \tag{3}$$

where V_i and L_i are molar flow rates of component i in the vapor and liquid phases (kmol·s^{-1}), respectively, and N_i^V and N_i^L are molar fluxes of component i in the liquid and vapor phases, respectively. The following relations exist with respect to mass conservation: $m_V = \Sigma V_i$, $m_L = \Sigma L_i$, and $N_i^V = N_i^L = N_i$.

An overall momentum balance on the liquid-vapor mixture in the axial direction can be developed from the force-

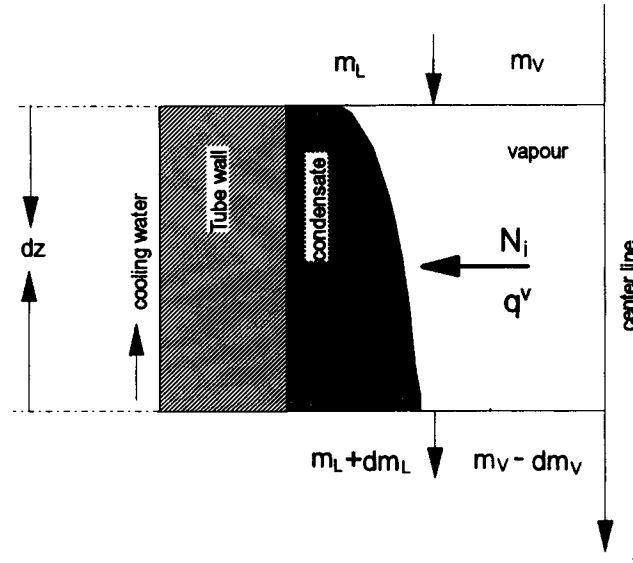

Figure 2. Mass transport during gas-liquid two-phase flow in a short section of a vertical tube.

Table 1. Energy Balance Equations

Energy Balance for the Vapor Phase $m_V c_P^V \frac{dT^V}{dA} = -q^V$	(4)
Energy Balance at the Liquid/Vapor Interface $h_o(T^I - T^c) = q^V + \Sigma N_i^L c_{Pi}^V (T^V - T^I) + \Sigma N_i^L \Delta h_i$	(5)
Energy Balance at the Wall $h_L(T^I - T^W) = h_{Wc}(T^W - T^c)$	(6)
Energy Balance for the Coolant $m_c c_P^c \frac{dT^c}{dA_{outs}} = -h_{Wc}(T^W - T^c)$	(7)

momentum balances on both the vapor and liquid phases. The resulting equation can be used to calculate the pressure drop for two-phase flow (Carey, 1992). However, the pressure drop is usually less than 3% of the total operating pressure in the heat exchanger (Jenkins et al., 1986, example 8), so the assumption of constant pressure throughout the exchanger could be made; thus this momentum equation was not required in our model.

Energy balance equations can be derived for both the vapor flow and coolant flow at the liquid/vapor interface, and at the tube wall, respectively. All energy balance equations are summarized in Table 1. In Eq. 4, q^V is the conductive heat flux out of the bulk vapor phase ($W \cdot m^{-2}$). The film model of simultaneous mass and heat transfer gives the expression for q^V (Krishna and Standart, 1979),

$$q^V = h_V \frac{\epsilon}{(e^\epsilon - 1)}(T^V - T^I) \tag{8}$$

where ϵ the heat-transfer rate factor is defined as

$$\epsilon = \Sigma N_i c_{Pi}^V / h_V \tag{9}$$

h_V is the zero-flux heat-transfer coefficient. $\epsilon/(e^\epsilon - 1)$ is known as Ackermann correction factor to correct the zero-flux coefficient for the effects of simultaneous mass transfer. In Eqs. 5 to 7, h_o is an overall heat-transfer coefficient accounting for the resistances to heat transfer in the condensate liquid, in the tube wall and in the coolant. h_L is the conductive heat-transfer coefficient in the condensate liquid, and h_{Wc} is the heat-transfer coefficient accounting for the heat-transfer resistances in the tube wall and in the coolant ($W \cdot m^{-2} \cdot K^{-1}$). The energy balance for the liquid phase can also be derived, so that the bulk liquid phase temperature T^L can be solved. Because the amount of condensed liquid is small (below 20 wt. %), the liquid film thickness throughout the exchanger is very thin and the temperature in the liquid phase can be approximated by $T^L = (T^I + T^W)/2$. In addition, the difference in the transfer area between the liquid/vapor interface and the tube inner wall is negligible.

Mass transfer in multicomponent vapor-gas mixtures

Although there are noncondensable components in the recycle gas mixture such as nitrogen and hydrogen, as suggested by Taylor and Krishna (1986), they are treated as condensable components in mass-transfer calculations. Hydrogen and nitrogen do not condense as pure components, but are sparingly soluble in the liquid phase. For the case of all condensable components (no component is completely noncondensable), the molar flux (N) can be calculated by Eq. 10

$$(N) = [\,k^V\,][\Xi](y^V - y^I) + N_t(y^V) \tag{10}$$

$[\,k^V\,]$ is a matrix of zero-flux mass-transfer coefficients ($m \cdot s^{-1}$), $[\Xi]$ is a matrix of correction factors to account for high flux of mass transfer, given by

$$[\Xi] = [\phi]\{\exp[\phi] - [I]\}^{-1} \tag{11}$$

where $[I]$ is an identity matrix. As mentioned in the introduction, many different film models might be employed to calculate the local mass-transfer rates in multicomponent systems. However, only the methods that take diffusion interaction effects into account are recommended. Here, the film model based on the linearized theory of Toor (1964) and Stewart and Prober (1964) was used, because it is considerably simpler in computation and gives indistinguishable results (Taylor and Krishna, 1993) compared with the method of Krishna and Standart (1976), which is based on an exact solution of the Maxwell-Stefan equations. By using the linearized method, the following relations can be utilized to compute the elements of mass-transfer matrix $[\,k^V\,]$ and matrix $[\phi]$

$$[\,k^V\,] = [M]^{-1}, \qquad [\phi] = N_t[M]$$

$$M_{ii} = \frac{\bar{y}_i}{\kappa_{in}} + \sum_{k=1(\neq i)}^{n} \frac{\bar{y}_k}{\kappa_{ik}}$$

$$M_{ij} = -\bar{y}_i\left(\frac{1}{\kappa_{ij}} - \frac{1}{\kappa_{in}}\right) \tag{12}$$

$[M]$ is a general matrix. In Eq. 12, $\bar{y}_i$ is the average of the interface composition y_i^I and the bulk vapor composition y_i^V. The binary mass-transfer coefficient κ_{ij} is defined as

$$\kappa_{ij} = (c_t D_{ij})/l \tag{13}$$

where c_t is the molar density of the vapor mixture ($kmol \cdot m^{-3}$), D_{ij} are Fickian diffusivities of binary mixtures ($m^2 \cdot s^{-1}$), and l is the liquid film thickness (m). An *a priori* estimate of the film thickness l must be available in order to evaluate binary mass-transfer coefficients κ_{ij}. For pure vapor condensation, an estimate of l can be obtained using empirical correlation methods (Numrich, 1990). For multicomponent condensation, both heat-transfer coefficients h_V ($W \cdot m^{-2} \cdot K^{-1}$) and binary mass-transfer coefficients κ_{ij} ($m \cdot s^{-1}$) are usually estimated using the j-factors of Chilton-Colburn analogy

$$j_H = \frac{h_V A_c}{m_V c_P}(Pr)^{2/3} = j_M = \frac{\kappa_{ij} A_c}{m_V}(Sc_{ij})^{2/3} = \frac{1}{2}f \tag{14}$$

In Eq. 14, Pr is the Prandtl Number, Sc_{ij} is the Schmidt number of binary gas pair i-j, and f is the friction factor. Many complicated correlations are available for calculating the friction factor f. However, in multicomponent condensation calculations, f is usually estimated by

$$f/2 = aRe^b \tag{15}$$

where a and b are correlation constants determined by fluid flow conditions. For Reynolds numbers over the range of $3\times 10^4 < Re < 10^6$, appropriate values of a and b are 0.023 and -0.2, respectively (Hines and Maddox, 1985).

As the level of turbulence increases, the diffusion interaction effect between different components decreases, because turbulent mass transport is not species-specific. However, if the Chilton-Colburn analogy is used to calculate mass-transfer coefficient κ_{ij}, it does not correctly reflect the diminished effect of molecular diffusion coupling, resulting from the increased level of turbulence, since the ratio of mass-transfer coefficients κ_{ij}/κ_{ii} is independent of the Reynolds number. Krishna (1982) developed a turbulent film model to include the contribution of turbulent mass transfer, which is called the turbulent eddy diffusivity model. Taylor et al. (1986) compared simulation results of Chilton-Colburn based film models and this turbulent eddy diffusivity model and found no significant difference for inlet Reynolds numbers up to 1,000,000. The detailed explanation of the reason for the success of the Chilton-Colburn analogy can be found in the analysis carried out by Taylor et al. (1986). Because the turbulent eddy diffusivity model is more complex than the Chilton-Colburn based film models, more computation time is required. Thus, the turbulent eddy diffusivity model will not be used in multicomponent mass-transfer calculations in this article.

Mass transfer in the liquid phase

The methods described above for calculating mass-transfer rates in the vapor/gas mixtures may, in principle, be extended to deal with the liquid phase. However, since the principal resistance to mass transfer resides in the vapor phase, a detailed model of mass-transfer processes in the liquid phase is not necessary. Usually one of two limiting cases of condensate behavior is used to calculate the composition in the liquid phase:

(1) The liquid phase is completely mixed with regard to composition. In this case, the following relation exists for the composition in the interface and in the bulk liquid phase from a material balance along the flow path

$$x_i^I = x_i^L = L_i/L \tag{16}$$

(2) The liquid phase is completely unmixed. In this case, the interfacial composition is given by

$$x_i^I = N_i/N_t \tag{17}$$

Investigations in the literature (Krishna et al., 1976; Webb and Sarsesai, 1981; Taylor et al., 1986) reveal that simulation results are generally insensitive to whichever extreme case is chosen if noncondensable gases are present in the vapor mixture. The completely mixed assumption (Eq. 16) is used in the current investigation.

Mass transfer at the liquid/vapor interface

Since the interface composition y_i^I on the vapor side is required to compute mass-flux N_i, it is necessary to set up an equation to relate y_i^I on the vapor and x_i^I on the liquid side. It is usually assumed that equilibrium prevails at the interface. Thus,

$$y_i^I = K_i x_i^I \quad i = 1,2,\ldots n \tag{18}$$

where K_i are equilibrium constants. In the analysis of vapor liquid equilibrium, K_i-values are key parameters and play a role that dominates the accuracy of the whole mass-transfer calculations. Estimation methods have been summarized by Reid et al. (1987). Using an equation of state (such as the Soave equation or the Peng-Robinson equation) to calculate K_i is highly recommended in our system.

Correlation methods for calculating the heat-transfer coefficient h_L in the condensate liquid film

For film condensation of vapor mixtures inside a vertical tube with noncondensing gases present, the overall heat-transfer resistance consists of the resistances to conductive heat transfer in the condensate and in the vapor-liquid boundary layer. The rate of heat transfer through the condensate layer is determined by the thickness of the condensate film, which is for condensation of pure vapors the only thermal resistance. A cocurrent downward vapor flow will tend to decrease the thermal resistance both by thinning the film and by increasing the likelihood of turbulence. For a highly turbulent downward vapor flow, the bulk motion of the core sweeps away noncondensable gases, leading to a lower buildup of the noncondensable gases at the interface. This factor will increase the interface temperature and result in less heat-transfer resistance as well. The heat-transfer coefficient in the condensate layer is therefore very much larger when there is significant vapor flow than when vapor flow is not present.

For condensation of a downward vapor flow inside a vertical tube at high velocity, the condensate flow is interfacial shear stress controlled; thus, the heat-transfer coefficient in the condensate layer is governed by interfacial shear stress. The description of heat-transfer enhancement by a significant gas flow is not sufficiently developed in the available literature. On the other hand, because of lack of experimental data, the reliabiity of the available correlation methods has not been investigated in a highly turbulent multicomponent system. The industrial data we have collected make it possible to evaluate different correlation methods. For comparison, correlations for both gravity controlled condensate flow and shear stress controlled condensate flow are given in Table 2.

If the velocity of the vapor flow is very low, the vapor shear force acting on the liquid/vapor interface is negligible, and the condensed liquid film falls under the influence of only gravity. In this case, the condensate flow is gravity controlled. In Table 2, Eqs. 19, 20 and 21 correspond to laminar wave-free flow and laminar wavy flow and turbulent flow, respec-

Table 2. Correlations of Estimating the Heat-Transfer Coefficient in the Condensate Liquid Film

			Reference
For Gravity Controlled Condensate Flow			
$h_L = 1.1\lambda_L Re^{(-1/3)}\left[\frac{\rho_L(\rho_L-\rho_V)g}{\eta_L^2}\right]^{1/3}$	$Re_L < 30$	(19)	Butterworth (1983) p. 2.6.2
$h_L = 0.756\lambda_L Re^{-0.22}\left[\frac{\rho_L(\rho_L-\rho_V)g}{\eta_L^2}\right]^{1/3}$	$Re_L > 30$	(20)	
$h_L = 0.023\lambda_L Re^{0.25} Pr_L^{0.5}\left[\frac{\rho_L(\rho_L-\rho_V)g}{\eta_L^2}\right]^{1/3}$	$Re_L \geq 1{,}600$, $Pr_L \leq 10$	(21)	
For Interfacial Shear Stress Controlled Condensate Flow			
$h_{L+} = 1.41 Re_L^{-1/2}(\tau_I^+)^{1/2}$	for laminar condensate flow	(22)	Butterworth (1983) p. 2.6.2
$\frac{h_{L+}}{(\tau_I^+)^{1/2}} = \left[\left(\frac{1.41}{Re_L^{1/2}}\right)^{\theta} + \left(\frac{0.071 Pr_L^{1/2}}{Re_L^{1/24}}\right)^{\theta}\right]^{1/\theta}$	for turbulent condensate flow	(23)	
where h_{L+}, the dimensionless heat-transfer coefficient is defined by			
$h_{L+} = \frac{h_L}{\lambda_L}\left[\frac{\eta_L^2}{\rho_L(\rho_L-\rho_V)g}\right]^{1/3}$		(24)	
$h_L = \lambda_L\left[\frac{\rho_L(\rho_L-\rho_V)g}{\eta_L^2}\right]\left[\left(0.31 Re_x^{-1.32} + \frac{Re_x^{2.4} Pr_L^{3.9}}{2.37\times 10^{14}}\right)^{1/3} + \frac{A_D Pr_L^{1.3}}{771.6}(Re_{ter} - Re_x)^{1.4} Re_x^{0.4}\right]^{1/2}$	for both laminar and turbulent condensate flow	(25)	Chen et al. (1987)

tively. In these three equations, the local Reynolds number of the condensate film Re_L is defined as

$$Re_L = \frac{4m_L}{\pi d\eta_L} \tag{26}$$

where d is the tube inside diameter (m), η_L is the viscosity of the liquid phase (Pa·s).

For interfacial shear stress controlled condensate flow, turbulent flow of the condensate film is initiated at much lower values of Re_L. The critical film Reynolds number for transition from laminar to turbulent is an important parameter and is believed to be reduced due to downward interfacial shear. For high and low interfacial shears, the critical film Reynolds number can be estimated by the following equations (Butterworth, 1983)

$$Re_c = 1{,}600 - 226(\tau_I^+)^3 \quad \text{for } \tau_I^+ \leq 9.04 \tag{27}$$

$$Re_c = 50 \quad \text{for } \tau_I^+ > 9.04 \tag{28}$$

In Eqs. 22, 23 and 27, τ_I^+ is a dimensionless interfacial shear stress, and $\theta = (Pr_L + 3)/2$. The choice between Eqs. 22 and 23 is governed by whether Re_L is less or greater than the critical film Reynolds number. Butterworth (1983) pointed out that Eq. 23 tends to overpredict the heat-transfer coefficient for $Pr_L > 10$. The typical value of Pr_L in our system is around 3.0.

More recently, Chen et al. (1987) have proposed a comprehensive film-condensation heat-transfer correlation based on analytical and theoretical results from the literature. For annular flow condensation in vertical tubes, the heat-transfer coefficient including the effects of gravity, interfacial waves, and interfacial shear in the condensate liquid film is given by Eq. 25, where A_D, Re_{ter} and Re_x are defined as

$$A_D = \frac{0.252\eta_L^{1.177}\eta_g^{0.156}}{d^2 g^{2/3}\rho_L^{0.553}\rho_g^{0.78}} \tag{29}$$

$$Re_{ter} = \frac{4(m_V + m_L)}{\pi\eta_L d} \tag{30}$$

$$Re_x = \frac{4m_V}{\pi\eta_L d} \tag{31}$$

Equation 25 agrees fairly well with the local condensation heat-transfer data obtained by Ueda et al. (1976).

Solution of Model Equations

The model equations are a set of differential and algebraic equations (Eqs. 2–7, 10 and 18). In these equations, there are intensive physical and transport properties, which are temperature and composition dependent. The model equations are highly nonlinear and must be solved numerically. Two kinds of methods are described in the literature to solve these equations: methods that use a tearing strategy (Krishna et al., 1976; Webb and McNaught, 1980), and simultaneous techniques based on Newton's method (Taylor et al., 1986). In methods that use a tearing strategy, at least two iterative loops are involved. For example, in the outer loop, a subset of variables (also called tearing variables) is iteratively solved first. Then the inner loop equations are iterated until convergence is obtained. The resulting inner loop solutions determine how the tearing variables are to be reestimated so that all the equations are satisfied exactly. In Newton's method (Taylor

Table 3. Model Equations for the jth Section of the Heat Exchanger

Material Balance for the Vapor Phase $F_i^V = V_{i,j-1} - V_{ij} - N_{ij}\Delta A_j = 0$	$i = 1,2,\ldots n$	(32)
Material Balance for the Liquid Phase $F_{n+i}^L = L_{i,j-1} - L_{ij} - N_{ij}\Delta A_j = 0$	$i = 1,2,\ldots n$	(33)
Rate Equations for Mass Transfer $F_{2n+i}^N = (N)_j - [M]_j^{-1}[\Phi]_j[e^{[\Phi]_j} - [I]^{-1}(\bar{y}^V - y^I)_j - N_{ij}(y^V)_j = 0$		(34)
Equilibrium Equations for the Interface $F_{3n-1+i}^I = K_{ij}x_{ij}^I - y_{ij}^I = 0$	$i = 1,2\ldots,n$	(35)
Energy Balance for the Vapor Phase $F_{4n} = \bar{m}_{Vj}c_{pj}^V(T_j^V - T_{j-1}^V) + h_{Vj}\frac{\epsilon_j}{e^{\epsilon_j}-1}(\bar{T}_j^V - T_j^I)\Delta A_j = 0$		(36)
Energy Balance at the Tube Wall $F_{4n+i} = h_{Lj}(T_j^I - T_j^W) - h_{Wcj}(T_j^I - \bar{T}_j^c) = 0$		(37)
Energy Balance for the Coolant $F_{4n+2} = m_c c_{pj}^c(T_{j-1}^c - T_j^c) + h_{Wcj}(T_j^W - \bar{T}_j^c)\Delta A_j = 0$		(38)
Energy Balance at the Vapor/Liquid Interface $F_{4n+3} = h_{Vj}\frac{\epsilon_j e^{\epsilon_j}}{e^{\epsilon_j}-1}(\bar{T}_j^V - T_j^I) + \Sigma N_{ij}\Delta h_i - h_{oj}(T_j^I - \bar{T}_j^c) = 0$		(39)

(Taylor et al., 1986), only one iterative loop is required. Given the initial guesses of all the unknowns, all of the model equations are solved simultaneously.

The heat exchanger is divided into a number of sections. In each section, the differential equations are replaced by finite difference approximations, so that all the model equations become algebraic equations. The resulting $4n+3$ model equations for the jth section of the heat exchanger are summarized in Table 3, which can be used to solve the $4n+3$ unknowns listed at the beginning of the model development section. Taylor et al. (1986) recommended that the bulk conditions within a heat-exchanger section ($\bar{T}_j^V$, $\bar{T}_j^c$, $\bar{y}_{ij}^V$, $\bar{x}_{ij}$, and $\bar{m}_{Vj}$) be determined using an average of the values at the beginning and at the end of the section, thus

$$\bar{T}_j^V = \left(T_j^V + T_{j-1}^V\right)/2 \qquad \bar{T}_j^c = (T_j^c + T_{j-1}^c)/2$$

$$\bar{y}_{ij}^V = (V_{ij}/m_{Vj} + V_{i,i-1}/m_{V,j-1})/2$$

$$\bar{x}_{ij} = (L_{ij}/m_{Lj} + L_{i,j-1}/m_{L,j-1})/2$$

$$\bar{m}_{Vj} = (m_{Vj} + m_{V,j-1})/2$$

The term $e^{[\Phi]}$ in Eq. 34 can be evaluated by a Taylor series expansion

$$e^{[\Phi]} = \sum_{i=0}^{\infty}\frac{[\Phi]^i}{i!} = [I] + [\Phi] + \frac{[\Phi]^2}{2!} + \ldots + \frac{[\Phi]^m}{m!} \quad (40)$$

Using Newton's method, the new prediction of unknowns (X_{k+1}) is given by a solution of the set of equations (F) (from Eqs. 32 to 39) linearized about the current estimate (X_k).

$$[J_k](X_{k+1} - X_k) = -(F_k) \quad (41)$$

where $[J_k]$ is the Jacobian matrix. A major difficulty when using Newton's method is the computation of Jacobian matrix $[J_k]$, since complete derivative information is difficult to obtain in analytical form. If finite differences are used to approximate those "unavailable" derivatives, many more physical property calculations are required. Taylor recommended the so-called hybrid method of Lucia and coworkers (Lucia and Macchietto, 1983; Taylor et al., 1983) to avoid this obstacle. In the hybrid method, the Jacobian matrix is split into two parts: $[C_k]$ and $[A_k]$.

$$[J_k] = [C_k] + [A_k] \quad (42)$$

Matrix $[C_k]$ contains all the partial derivatives of $[J_k]$ that can be obtained analytically. $[A_k]$ is made up of any partial derivatives whose analytical expressions are difficult to obtain. $[A_k]$ can be estimated by finite difference approximations or one of Quasi-Newton methods. When using a Quasi-Newton method, $[A_k]$ can be updated from an initial approximation to $[J]$ based on the information on the changes in (X) and (F).

The hybrid method is certainly superior to the tearing method. However, in the current system, many of the physical properties and parameters are strongly dependent on temperature and composition. The hybrid method occasionally failed to reach convergence because of inappropriate initial guess of unknowns or inappropriate initial approximation of $[A_0]$. The choice of whether some partial derivatives should be included in $[A_k]$ does not only depend on whether or not the analytical form of partial derivatives is difficult to obtain. If some important derivatives are not included in $[C_k]$, convergence problems can occur. However, convergence is not affected at all by assuming some unimportant derivatives to be zero. We have observed that convergence is hard to obtain using the hybrid method for our system.

Unfortunately, even when a complete analytical Jacobian is available, Newton's method can have convergence difficulties if the initial guess is not sufficiently close to the root. If the step size is not small enough, then the solution in the current section of the heat exchanger is not good enough as an initial estimate for the unknowns of the subsequent section. To overcome this problem, we have resorted to a globally convergent method for solving nonlinear systems of equations.

Globally convergent methods

A global method is one that converges to a solution from almost any starting point. Newton's method can be "adapted" to an algorithm that will guarantee some progress towards the solution at each iteration (Press et al., 1992). For a set of equations

$$F(X) = 0 \tag{43}$$

the Newton step is

$$X_{\text{new}} = X_{\text{old}} + \delta X \tag{44}$$

where

$$\delta X = -[J]^{-1} \cdot (F)$$

How does one decide whether to accept the Newton step δX? A reasonable strategy is to require that the step decreases the sum of squared discrepancies, $[F]^2 = F \cdot F$. This is equivalent to minimizing

$$f = F \cdot F/2 \tag{45}$$

A good strategy is to always try the full Newton step first, since once the vicinity of the solution is reached, quadratic convergence will be obtained. However, at each iteration one should check whether the proposed step reduces f. If not, backtrack along the Newton direction until an acceptable step is obtained. A detailed description of globally convergent methods is given by Press et al. (1992).

Using this globally convergent method, there is no problem with poor initial guesses and the choice of step size in most cases. As this method essentially minimizes f by taking Newton steps designed to bring F to zero, which is not equivalent to minimizing f by taking Newton steps designed to bring ∇f to zero, this method can still occasionally fail by landing on a local minimum of f.

For our model equations, the typical unscaled values of discrepancy function F_i vary from the magnitude of 10^{-4} to 10^{+5}, and the resulting Jacobian matrix $[J]$ is ill-conditioned leading to very slow convergence or no convergence at all. Convergence problems were alleviated by scaling values of both the unknown variable X_i and discrepancy function F_i so that their typical values are all of order unity. The detailed calculation procedure can be found in the thesis of Jiang (1996).

Simulation Results and Discussions

It has been shown in many studies (Sparrow et al., 1967; Denny et al., 1971; Kim and Corradini, 1990) that if there are noncondensable gases present, then the main resistance to heat transfer resides in the vapor-liquid boundary layer. The influence of highly turbulent co-current vapor phase flow makes the heat-transfer resistance in the liquid film even smaller. Using the three different correlation methods summarized in Table 2 to calculate the local heat-transfer coefficient in the condensate layer, we will compare the simulation results and see how the calculated temperatures at the bottom of the exchanger compare to the industrial data. Three

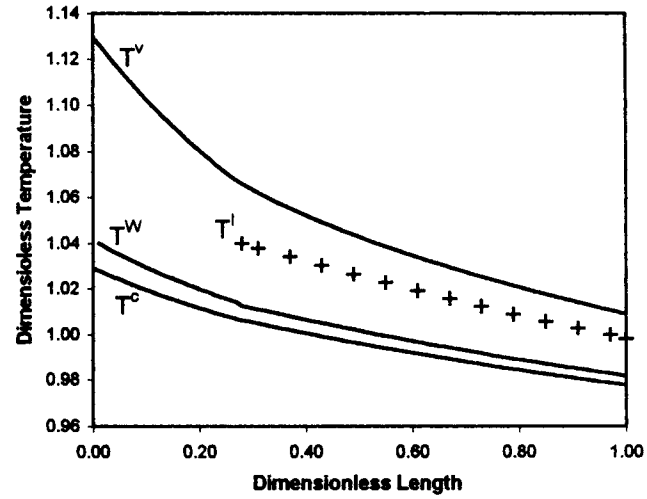

Figure 3. Temperature distribution in the heat exchanger.

h_L is estimated by Eq. 20, which is used for gravity controlled condensate flow.

sets of temperature profiles shown in Figures 3, 4 and 5 correspond to different methods for estimating h_L: (1) the method for gravity controlled condensate flow (Eq. 20); (2) the Butterworth (1983) method for shear stress controlled condensate flow (Eq. 22); and (3) the Chen et al. (1987) method for shear stress controlled condensate flow (Eq. 25).

First, look at the relationships among T^V, T^I and T^W in these three graphs. If the interfacial shear stress is not considered and Eq. 20 is used, it can be seen in Figure 3 that the calculated heat-transfer resistance in the liquid film is even higher than in the vapor-liquid boundary layer, because the difference $(T^I - T^W)$ between the wall temperature and interface temperature is larger than the difference $(T^V - T^I)$ between the bulk vapor phase temperature and interface temperature. Hence, it can be seen that inappropriate temperature profiles are obtained when the interfacial shear

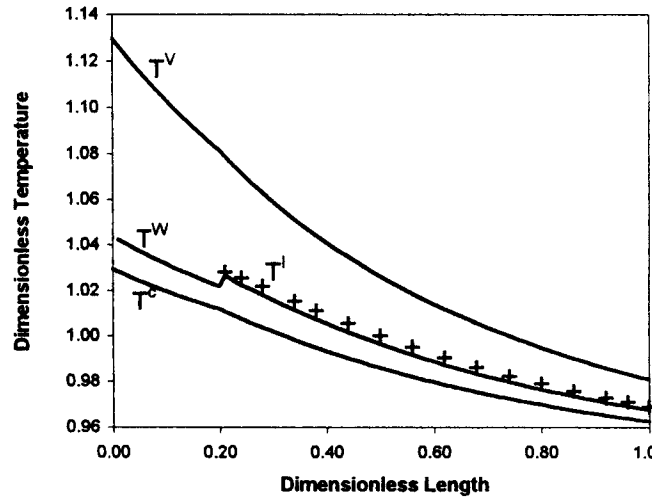

Figure 4. Temperature distribution in the heat exchanger.

h_L is estimated by the method of Butterworth (1983), Eq. 22, which is used for shear stress controlled condensate flow.

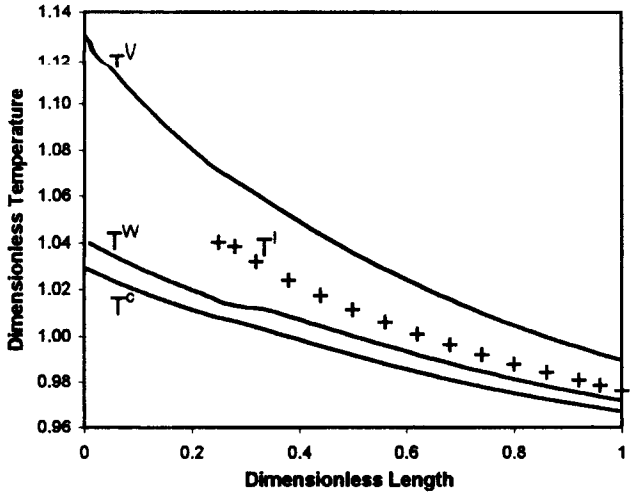

Figure 5. Temperature distribution in the heat exchanger.

h_L is estimated by the method of Chen et al. (1987), Eq. 25, which is used for shear stress controlled condensate flow.

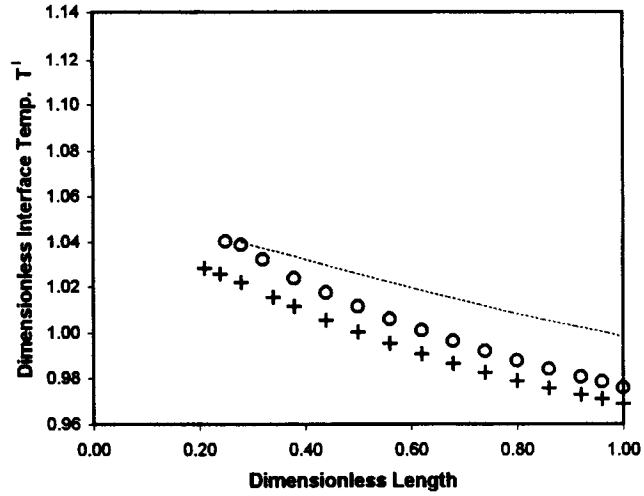

Figure 6. Interface temperature distribution along the length of the exchanger.

(---) Equation 20 for gravity controlled condensate flow; (oo) Eq. 25 and (+ +) Eq. 22 for shear stress controlled condensate flow.

stress is not considered. Using Butterworth's (1983) method for shear stress controlled condensate flow (Eq. 22), the curves (Figure 4) representing interface temperature T^I and the wall temperature T^W are very much closer to each other, indicating that the heat-transfer resistance in the liquid film is very small. At the point where condensation begins, the wall temperature T^W suddenly jumps to a high value and then decreases subsequently. This is because the value of h_L calculated by Eq. 22 is so high at the very beginning of condensation that the resulting heat-transfer resistance in the liquid layer is very small. However, condensation calculations require that the gas mixture condenses at a higher temperature. The ultimate result is that T^W jumps to a high value to satisfy the condensation requirement. At the beginning of condensation, since only a tiny amount of condensed liquid is present, high vapor shear stress may result in high liquid entrainment or breakdown of a continuous liquid film. Rosson and Meyers (1965) suggested that upper and lower portions of the tube be treated separately. In fact, calculations show that the condensate flow in our system is turbulent; thus, Eq. 23 should be used to estimate h_L when condensation begins. However, if Eq. 23 is employed, the curves representing T^W and T^I cannot be distinguished at all. And there will be a higher jump for T^W at the starting point of condensation. Obviously, Butterworth's (1983) correlation method cannot correctly characterize the heat-transfer resistance in the liquid film at the beginning of condensation. However, this simulation result actually supports the conclusion made by Siddique et al. (1993) that the liquid-vapor boundary layer is the controlling resistance for highly turbulent condensation. Neglecting the liquid film heat-transfer resistance, the models they developed that predict local overall heat-transfer coefficients correlate reasonably well with their experimental data and can be used to estimate local overall heat-transfer coefficients for the range of conditions used in their experiments.

If Chen et al.'s (1987) correlation method (Eq. 25) is used, the resulting temperature profiles are shown in Figure 5. It can be seen that during the initial period of condensation, there is little difference between $(T^I - T^W)$ and $(T^V - T^I)$. In other words, the heat-transfer resistance in the liquid layer and in the vapor-liquid boundary layer is almost the same. After the initial period of condensation, the interfacial temperature T^I moves close to the wall temperature T^W, i.e., the resistance to heat transfer in the vapor-liquid boundary layer becomes greater than in the liquid layer. This is because the condensate flow initially is laminar and can be very different from the turbulent flow in the remaining period of condensation process. The tube wall temperature profile T^W is much smoother around the starting point of condensation than the T^W curve in Figure 4. For comparison, the three interfacial temperature curves are plotted on the same graph in Figure 6. It can be seen that the starting dewpoint temperature obtained by using Chen et al.'s method (Eq. 25) is very close to the temperature calculated by the method for gravity controlled condensate flow (Eq. 20). As the condensation continues, the T^I curve obtained by Chen et al.'s method moves closer to the T^I curve obtained by Butterworth et al.'s method. It appears from Figure 6 that Chen et al.'s method can correctly characterize the transition process of the condensate flow from laminar to turbulent flow under co-current turbulent vapor phase flow.

At the bottom of the heat exchanger, the available industrial data include the outlet vapor phase temperature T^V_{out}, and the inlet cooling water temperature T^c_{in}. Unfortunately, the industrial data are proprietary, and the plant data used to perform simulations cannot be provided. Here, the simulation results are only used to show how the model works when predicting the plant data. The three pairs of curves representing T^V and T^c corresponding to these three kinds of methods of calculating h_L are displayed in Figure 7, and are compared with industrial data shown by open circles. From Figure 7, it can be seen that at the bottom of the exchanger, the calculated T^V_{out} and T^c_{in} by using Eq. 20 are much higher than the industrial data. The temperature difference $(T^V_{\text{out}} - T^c_{\text{in}})$ is also larger than the corresponding industrial data. The correlation method for gravity controlled condensate flow

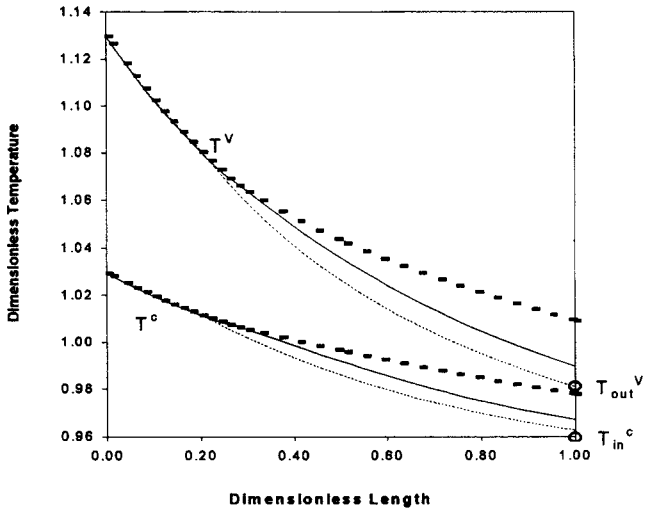

Figure 7. Temperature distribution along the length of the exchanger—comparing simulation results with industrial data.

— — — h_L was estimated by the correlation for gravity controlled condensate flow (Eq. 20); —— h_L was calculated by Chen et al.'s (1987) method (Eq. 25); and - - - - h_L was calculated by Butterworth et al.'s (1983) method (Eq. 22); o are the industrial temperature measurements at the bottom of the exchanger.

failed to describe the heat-transfer coefficient in the liquid layer. When Eq. 25 is used, the resulting temperatures T^V_{out} and T^c_{in} are closer, yet still slightly higher than the industrial data. The temperature difference $(T^V_{out} - T^c_{in})$ obtained by Eq. 25 is very close to the industrial value. If Eq. 22 is utilized, the best agreement between the simulation results and the industrial data can be obtained among these three kinds of correlation methods. However, the resulting value of the temperature difference $(T^V_{out} - T^c_{in})$ is slightly smaller than the industrial value, but is predicted within an accuracy of ± 2.0°C.

From the above analysis, it can be seen that Chen et al.'s method gives a better estimation of the heat-transfer coefficient at the initial stage of condensation. However, it seems that Butterworth's method (Eq. 22) gives a better estimation of the overall heat-transfer coefficient even though Eq. 22 should be used for laminar condensate flow according to Butterworth (1983).

Comparison with equilibrium methods

Theoretically, there is no doubt that nonequilibrium methods are more soundly based than equilibrium methods. However, because of their simplicity, equilibrium methods are favored methods for industrial applications, especially for totally condensable mixtures. For partial condensers, as pointed out by Bell and Ghaly (1973), a critical aspect of the problem is the resistance to mass transfer in the vapor phase. Two techniques are available in equilibrium methods. One of the techniques is Kern's (1950) method, which ignores any vapor phase resistance to heat transfer and which can lead to severe underdesign of condensers (Webb and McNaught, 1980). The other technique is Bell and Ghaly's (1973) method, which does not ignore heat-transfer resistance in the vapor phase, but tries to overestimate the heat-transfer resistance to compensate for the error introduced by neglecting the mass-transfer resistance. Figure 8 gives a comparison of temperature profiles for Kern's method, Bell and Ghaly's method, and the nonequilibrium method described in this work. Kern's method shows that at the bottom of the exchanger, the vapor phase temperature T^V_{out} and coolant water temperature T^c_{in} are much lower than the plant data, while the results obtained by Bell and Ghaly's method are closer to the plant data but still inferior to the nonequilibrium method. Comparing the temperature profiles, it can be seen that the temperature curves of the two equilibrium methods diverge around 0.23 dimensionless distance from the temperature lines of the nonequilibrium method. That is because condensation occurs much earlier for nonequilibrium methods since the two phases are assumed in equilibrium at the interface temperature, not at the bulk vapor phase temperature as presumed in equilibrium methods. There are breaks in the temperature curves at the starting point of condensation for the two equilibrium techniques. When condensation occurs, much larger amounts of heat must be released which requires larger heat-transfer area and higher driving forces, i.e., greater temperature difference of $(T^V - T^c)$. Since the heat-transfer resistance in the vapor phase is considered in Bell and Ghaly's method, the resulting overall heat-transfer coefficient is smaller compared to that of Kern's method. That is why even bigger breaks exist in the temperature lines of Bell and Bhaly's method. To compare how equilibrium and nonequilibrium methods work,

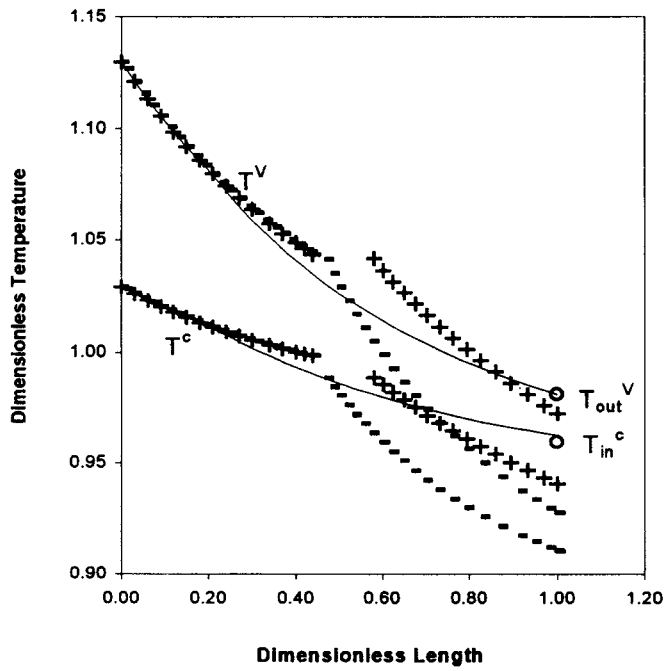

Figure 8. Temperature distribution along the length of the exchanger—comparing simulation results of equilibrium methods and nonequilibrium methods.

— — — Kern's method (1950); + + + the Bell and Ghaly's method; —— nonequilibrium method (h_L was calculated by Butterworth et al.'s (1983) method); o are the industrial temperature measurements at the bottom of the exchanger.

Table 4. Comparison of Outlet Conditions for the Kern, the Bell and Ghaly and the Nonequilibrium Methods

Outlet Conditions	Kern	Bell and Ghaly	Nonequilibrium
Vapor temp., T_{out}^V, K	17.2 K < T_{out}^V (plant)	3.0 K < T_{out}^V (plant)	0.2 K < T_{out}^V (plant)
Coolant temp., T_{in}^c, K	15.7 K < T_{in}^c (plant)	6.0 K < T_{in}^c (plant)	1.0 K > T_{in}^c (plant)
Heat removed/tube, kJ/s	45.027	31.213	29.253
Total condensation rate, wt. %	24.87	15.89	13.47

Table 4 shows important outlet conditions for these three methods.

Sensitivity to errors and fluctuations in plant data

The industrial data used in this work are averages of 70 h of stable plant operation. In this 70 h operating period, the most significant data fluctuation was found in gas-flow rates. The maximum uncertainty in gas-flow rates is about 10%. The sensitivity analysis has been done by perturbing the conditions at the top of the heat exchanger individually and monitoring the resulting temperature values at the bottom of the heat exchanger, which are unfortunately the only available industrial measurements. The results of sensitivity analysis are shown in Table 5. The temperatures (T_{out}^V and T_{in}^c) at the bottom of the exchanger are not particularly sensitive to the random measurements errors of the conditions at the top of the exchanger.

Conclusions

Nonequilibrium methods for multicomponent condensation are applied to simulate a vertical single pass shell-and-tube heat exchanger in a polyethylene reactor system operated in condensing mode. The operating pressure in the exchanger is assumed constant. The local mass- and heat-transfer coefficients are functions of temperature and composition, and are estimated using appropriate local average values. The differential mass and energy balance equations are approximated by finite difference equations. Methods for solving the resulting highly nonlinear algebraic equations are discussed. It was found that convergence is difficult to obtain in our system by using either the hybrid methods or Newton's methods. A practical way of solving the set of algebraic equations was a technique combining the rapid local convergence of Newton's method with a globally convergent strategy. Techniques for estimating the local heat-transfer coefficients in the liquid film layer have been investigated. Compared to industrial data, the best agreement was obtained when h_L was estimated by Butterworth's (1983) correlation method. Chen et al.'s (1987) method provided a better description of the transition process of condensate flow from initially laminar flow to turbulent flow. The results of sensitivity analysis for random measurement fluctuations in industrial data support our conclusion that this model gives reasonable agreement between industrial data and simulation results. Effects of operating conditions of the heat exchanger and reactor system on the heat removal rate, and especially effects of noncondensable gas composition on condensation heat transfer will be the focus of a subsequent article.

Table 5. Sensitivity Analysis Regarding the Gross and Random Errors of Plant Data

Conditions	Uncertainty	T_{out}^V	T_{in}^c
Gas-flow rate	+10%	−1.7 K	−3.1 K
	−10%	+1.8 K	+3.0 K
Inlet vapor temp. T_{in}^V	+2.0 K	+0.8 K	+1.1 K
	−2.0 K	−0.8 K	−1.2 K
Outlet coolant temp. T_{out}^c	+2.0 K	+3.5 K	+3.8 K
	−2.0 K	−3.3 K	−3.7 K
Isohexane mole fraction	+8.15%	−0.4 K	−0.6 K
	−8.15%	+0.7 K	+0.7 K
Ethylene mole fraction	+8.15%	+0.4 K	+0.4 K
	−8.15%	−0.3 K	−1.4 K

Acknowledgment

The authors wish to thank Queen's University, the School of Graduate Studies and Research, and the Natural Science and Engineering Research Council of Canada for support of this research.

Notation

A_c = cross section area of the tube, m^2
A_{outs} = surface area of the tube outside, m^2
$[A]$ = approximated part of Jacobian matrix
A = interfacial area, m^2
c_P = molar heat capacity, $J \cdot kmol^{-1} \cdot K^{-1}$
$[C]$ = computed part of Jacobian matrix
(F) = vector of dependent functions (equations)
g = acceleration of gravity, $m \cdot s^{-2}$
h = heat-transfer coefficient, $W \cdot m^{-2} \cdot K^{-1}$
h_{L+} = dimensionless heat-transfer coefficient in the liquid layer
Δh_i = latent heat of vaporization of component i, J/kmol
j_H = Chilton-Colburn j-factor for the heat transfer
j_M = Chilton-Colburn j-factor for mass transfer
m_c = coolant mass-flow rate, $kg \cdot s^{-1}$
M_t = total molar flow rate of the entering recycle gas mixture, kmol $\cdot s^{-1}$
Re_c = critical Reynolds number
x = mole fraction in liquid phase
(X) = vector of independent variables
y = mole fraction in vapor phase
Y_i = mole fraction of component i in the entering recycle gas mixture
z = axial coordinate, m
λ = thermal conductivity, $W \cdot m^{-2} \cdot K^{-1}$
ρ = density, $kg \cdot m^{-3}$

Subscripts and/or superscripts

i, j, k = component indexes or section numbers, j only
$\cdot$ = overall parameter
t = total value

Literature Cited

Bandrowski, J., and A. Kubaczka, "On the Condensation of Multicomponent Vapors in the Presence of Inert Gases," *Int. J. Heat Mass Transf.*, **24**, 147 (1981).

Bell, K. J., and M. A. Ghaly, "An Approximate Generalized Design Method for Multicomponent/Partial Condensers," *AIChE Symp. Ser.*, **69**, 72 (1973).
Burdett, I. D., "The Union Carbide UNIPOL Process: Polymerization of Olefins in a Gas-Phase Fluidized Bed," AIChE meeting, Washington, DC (Nov. 27–Dec. 2, 1988).
Butterworth, D., *Heat Exchanger Design Handbook*, E. H. Schlünder, ed., Hemisphere, Washington, DC, p. 2.6.2 (1983).
Carey, V. P., *Liquid-Vapour Phase-Changer Phenomena (An Introduction to the Thermophysics of Vaporization and Condensation Processes in Heat Transfer Equipment)*, Hemisphere Publishing Corp., Washington, Philadelphia and London, p. 412 (1992).
Chen, S. L., F. M. Gerner, and C. L. Tien, "General Film Condensation Correlations," *Exp. J. Heat Transf.*, **1**, 93 (1987).
Choi, K. Y., and W. H. Ray, "Recent Developments in Transition Metal Catalyzed Olefin Polymerization—A Survey. I. Ethylene Polymerization," *J. Macromol. Sci. Rev. Macromol. Chem. Phys.*, **C25**(1), 1 (1985).
Colburn, A. P., and T. B. Drew, "The Condensation of Mixed Vapours," *Trans. Amer. Chem. Eng.*, **33**, 197 (1937).
Denny, V. E., A. F. Mills, and V. J. Jusionis, "Laminar Film Condensation from a Steam-Air Mixture Undergoing Forced Flow Down a Vertical Surface," *J. Heat Transf.*, **93**, 297 (1971).
Hines, A. L., and R. N. Maddox, *Mass Transfer Fundamentals and Applications*, Prentice-Hall, Inc., Englewood Cliffs, NJ, p. 179 (1985).
Jenkins, III, J. M., R. L. Jones, T. M. Jones, and S. Beret, "Method for Fluidized Bed Polymerization," United States Patent Number 4588790 (May 13, 1986).
Jiang, Y., "Nonequilibrium Modeling of Multicomponent Condensation in a Vertical Heat Exchanger of a Polyethylene Reactor," PhD Thesis, Queen's Univ., Kingston, Ontario, Canada (1997).
Kern, D. Q., *Process Heat Transfer*, McGraw-Hill: New York (1950).
Kholpanov, L. P., and E. Ya. Kenig, "Coupled Mass and Heat Transfer in a Multicomponent Turbulent Falling Liquid Film," *Int. J. Heat Mass Transf.*, **36**(14), 3647 (1993).
Kim, M. H., and M. L. Corradini, "Modeling of Condensation Heat Transfer in a Reactor," *Nucl. Eng. Des.*, **118**, 193 (1990).
Krishna, R., C. B. Panchal, D. R. Webb, and I. Coward, "An Ackermann-Colburn and Drew Type Analysis for Condensation of Multicomponent Mixtures," *Lett. Heat Mass Transfer*, **3**, 163 (1976).
Krishna, R., and G. L. Standart, "A Multicomponent Film Model Incorporating a General Matrix Method of Solution to the Maxwell-Stefan Equations," *AIChE J.*, **22**(2), 383 (1976).
Krishna, R., and C. B. Panchal, "Condensation of a Binary Vapour Mixture in the Presence of an Inert Gas," *Chem. Eng. Sci.*, **32**, 741 (1977).
Krishna, R., "A Simplified Mass Transfer Analysis for Multicomponent Condensation," *Lett. Heat Mass Transf.*, **6**, 439 (1979).
Krishna, R., "A Turbulent Film Model for Multicomponent Mass Transfer," *The Chem. Eng. J.*, **24**, 163 (1982).
Krishna, R., "Effect of Nature and Composition of Inert Gas on Binary Vapour Condensation," *Lett. Heat Mass Transf.*, **6**, 137 (1979).
Krishna, R., and G. L. Standart, "Mass and Energy Transfer in Multicomponent Systems," *Chem. Eng. Commun.*, **3**, 201 (1979).
Krishna, R., and R. Taylor, *Handbook of Heat and Mass Transfer*, N. C. Cheremisinoff, ed., Gulf Publishing Company, Houston (1986).
Lucia, A., and S. Macchietto, "A New Approach to Approximation of Quantities Involving Physical Properties Derivatives in Equation-Oriented Process Design," *AIChE J.*, **29**, 705 (1983).
McNaught, J. M., *Heat Exchangers—Theory and Practice*, J. Taborek, G. F. Hewitt, and N. Afgan, eds., Hemisphere Publishing Corp., Washington, DC (1983).
Numrich, R., "Influence of Gas Flow on Heat Transfer in Film Condensation," *Chem. Eng. Technol.*, **13**, 136 (1990).
Press, W. H., S. A. Teukolsky, W. T. Vetterling, and B. P. Flannery, *Numerical Recipes in Fortran: the Art of Scientific Computing*, 2nd ed., Cambridge Univ. Press (1992).
Reid, R. C., J. Prausnitz, and B. E. Poling, *The Properties of Gases and Liquid*, McGraw-Hill, Toronto (1987).
Rosson, H. F., and J. A. Meyers, "Point Values of Condensing Film Coefficients Inside a Horizontal Tube," *Chem. Eng. Prog. Symp. Ser.*, **61**(59), 190 (1965).
Sardesai, R. G., "Studies in Condensation," PhD Thesis. University of Manchester Institute of Science and Technology (1979).
Schrodt, J. T., "Simultaneous Heat and Mass Transfer from Multicomponent Condensing Vapour-Gas Systems," *AIChE J.*, **19**(4), 753 (1973).
Siddique, M., M. W. Golay, and M. S. Kazimi, "Local Heat Transfer Coefficients for Forced-Convection Condensation of Stream in a Vertical Tube in the Presence of a Noncondensable Gas," *Nucl. Technol.*, **102**, 386 (1993).
Silver, L., "Gas Cooling with Aqueous Condensation," *Trans. Inst. Chem. Eng.*, **25**, 30 (1947).
Sparrow, E. M., W. J. Minkowycz, and M. Saddy, "Forced Convection Condensation in the Presence of Noncondensables and Interfacial Resistance," *Int. J. Heat Mass Transf.*, **10**, 1829 (1967).
Stewart, W. E., and R. Prober, "Matrix Calculation of Multicomponent Mass Transfer in Isothermal Systems," *Ind. Eng. Chem. Fundam.*, **3**, 224 (1964).
Taitel, Y., and A. Tamir, "Film Condensation of Multicomponent Mixtures," *Int. J. Multiphase Flow*, **1**, 697 (1974).
Tamir, A., and J. C. Merchuk, "Verification of a Theoretical Model for Multicomponent Condensation," *The Chem. Eng. J.*, **17**, 125 (1979).
Taylor, R., and L. W. Smith, "On Some Explicit Approximate Solutions of the Maxwell-Stefan Equations for the Multicomponent Film Model," *Chem. Eng. Commun.*, **14**, 361 (1982).
Taylor, R., A. Lucia, and R. Krishnamurthy, "A Newton-Like Algorithm for the Efficient Estimation of Rates of Multicomponent Condensation by a Film Model," *Inst. Chem. Eng. Symp. Ser.*, **75**, 380 (1983).
Taylor, R. R., Krishnamurthy, and J. S. Furno, "Condensation of Vapour Mixtures. 1. Nonequilibrium Models and Design Procedures," *Ind. Eng. Chem. Process Des. Dev.*, **25**, 83 (1986).
Taylor, R., and R. Krishna, *Multicomponent Mass Transfer*, Wiley, New York (1993).
Taylor, R., and M. K. Noah, "Simulation of Binary, Vapor Condensation in the Presence of an Inert Gas," *Lett. Heat and Mass Transfer*, **9**, 463 (1982).
Toor, H. L., "Solution of the Linearized Equations of Multicomponent Mass Transfer: II. Matrix Methods," *AIChE J.*, **10**(4), 460 (1964).
Ueda, T., T. Kubo, and M. Inoue, "Heat Transfer for Steam Condensing Inside a Vertical Tube," *Proc. Int. Heat Transfer Conf.*, **3**, 304 (1976).
Webb, D. R., and J. M. McNaught, *Development in Heat Exchanger Technology*, D. R. Chisoim, ed., Applied Science Publishers, Barking, England (1980).
Webb, D. R., and R. G. Sardesai, "Verification of Multicomponent Mass Transfer Models for Condensation Inside a Vertical Tube," *Int. J. Multiphase Flow*, **7**, 507 (1981).

Manuscript received Feb. 12, 1996, and revision received June 25, 1996.